Retrospective Clinical Research Report

Journal of INTERNATIONAL MEDICAL RESEARCH

Journal of International Medical Research
49(9) 1–11
© The Author(s) 2021
Article reuse guidelines:
sagepub.com/journals-permissions
DOI: 10.1177/03000605211039471
journals.sagepub.com/home/imr
SAGE

Expression and related mechanisms of miR-330-3p and S100B in an animal model of cartilage injury

Wenming Wu[1] and Dongming Liang[2]

Abstract

Objective: To investigate the roles of and relationship between microRNA (miR)-330-3p and S100 calcium-binding protein B (S100B) in an animal model of cartilage injury.

Methods: This study included 30 New Zealand male rabbits randomly divided into three groups: an intervention group, a model group and a sham surgery control group. Modelling was performed in the intervention and model groups, but in the sham surgery group, only the skin was cut. After modelling, the intervention and model groups were injected with the miR-330-3p overexpression vector GV268-miR-330-3p or the control GV268-N-ODN vector, respectively, twice a week for 7 weeks.

Results: Levels of interleukin-1β and tumour necrosis factor-α in the synovial fluid were significantly higher in the model group than in the intervention and control groups. The level of miR-330-3p in the cartilage tissue was significantly higher in the control group than in the model group but it was significantly lower compared with the intervention group. Levels of S100B, fibroblast growth factor receptor 1 and fibroblast growth factor-2 in the cartilage tissue of rabbits in the model group were significantly higher compared with the control and intervention groups.

Conclusion: These findings demonstrate that the upregulation of miR-330-3p can inhibit the expression of S100B.

Keywords

Interleukin-1β, tumour necrosis factor-α, fibroblast growth factor-2/fibroblast growth factor receptor 1 signalling

Date received: 8 December 2020; accepted: 26 July 2021

[1]Department of Orthopaedics, Beijing Ditan Hospital, Capital Medical University, Beijing, China
[2]Lirimax (Tianjin) Medical Technical Co., Ltd, Tianjin, China

Corresponding author:
Dongming Liang, Lirimax (Tianjin) Medical Technical Co., Ltd, 2 Fada Road, Wuqing District, Tianjin, 301700, China.
Email: ytg0g1@163.com

Creative Commons Non Commercial CC BY-NC: This article is distributed under the terms of the Creative Commons Attribution-NonCommercial 4.0 License (https://creativecommons.org/licenses/by-nc/4.0/) which permits non-commercial use, reproduction and distribution of the work without further permission provided the original work is attributed as specified on the SAGE and Open Access pages (https://us.sagepub.com/en-us/nam/open-access-at-sage).

Introduction

The primary role of articular cartilage is to reduce friction between the articular surfaces during movement.[1] Sprains and weight overload can cause damage to cartilage and subchondral bone.[2] Research has shown that a lack of blood supply and neuromodulation lead to insufficient self-repair of cartilage joints.[3] Other research has shown that when the diameter of the cartilage injury is >6 mm, the bone wall and articular cartilage around the injury are subsequently damaged.[4] Such damage is observed in patients with severe conditions, eventually leading to osteoarthritis (OA).[5]

The incidence of OA in patients aged >55 years is >44%.[6] OA can seriously affect the patient's quality of life.[7] At present, the clinical treatments of OA mainly focus on joint replacement. Although this approach has good clinical efficacy, it often increases the mental and economic burdens of patients.[8] Therefore, blocking cartilage injury with preventive treatment is a far superior option.

MicroRNAs (miRNAs) are transcribed into primary miRNAs by RNA polymerase II in the nucleus.[9] They are then processed into stem-loop structure precursor miRNAs of 60–100 nucleotides (nts) in length and transported to the cytoplasm where they are cleaved into mature miRNAs by Dicer.[10] miRNAs can inhibit the translation and transcription of target genes by binding to the 3′ untranslated regions (UTR) of their target gene mRNAs.[11] S100 calcium-binding protein B (S100B) is an important member of the S100 calcium-binding protein family.[12] S100B is closely associated with proliferation, apoptosis and differentiation.[13] A previous study found that S100B can regulate the inflammatory response during OA through fibroblast growth factor receptor 1 (FGFR1) signalling.[14]

Since inflammatory processes play a fundamental role in the damage of articular tissues, many *in vitro* and *in vivo* studies have examined the contribution of components of the nuclear factor-κB (NF-κB) signalling pathway to the pathogenesis of various cartilage injury, in particular, of OA.[15] The NF-κB signalling network is an important component of miRNA and S100 signalling in cartilage injury.[16] NF-κB inhibition is a rational objective in the treatment of rheumatic diseases such as OA.[17] Nonsteroidal anti-inflammatory drugs, nutraceuticals, natural products, probiotics and chondroitin sulfate have been shown to decrease NF-κB activation and proinflammatory cytokines.[18,19]

The study used the online the target gene software Targetscan to determine that miR-330-3p may target a gene that binds to S100B. The aim of the present study was to investigate the expression and related mechanisms of miR-330-3p and S100B in an animal model of cartilage damage caused by osteoarthritis in order to identify potential therapeutic targets for the clinic.

Materials and methods

Animals

A total of 30 New Zealand male rabbits (China Jinan Jinfeng Experimental Animal Co., Ltd. Jinan, China) aged 4 months and weighing 3.5 ± 0.3 kg were included in the study. After purchase, they were transferred to the animal laboratory and kept in separate cages for 1 week. The animals were kept way from sources of strong light and loud noises. They were maintained under a 12-h light/12-h dark cycle and had free access to food and water. All applicable international, national and/or institutional guidelines for the care and use of animals were followed, including the Guidelines for Ethical Conduct in the Care and Use of Animals Developed by the American Psychological Association's Committee on Animal Research and Ethics (CARE).[20]

This study was approved by the Ethics Committee of Beijing Ditan Hospital, Capital Medical University, Beijing, China (no. NCT02156327).

Animal model

The New Zealand rabbits were fasted for 12 h and then anaesthetized with urethane (200 g/l, 5 ml/kg) from the ear vein before modelling. They were divided into three groups according to a random number table, with 10 rabbits in each group: the intervention group, the model group and the sham surgery group. A cartilage injury model was established in the intervention and model groups.[21] The specific protocol was as follows. The right hind limbs were prepared under aseptic conditions. The knee joint was longitudinally cut 2 cm outside the tibia and the tissues were peeled off layer-by-layer until the femoral trochlear joint surface was exposed. A cartilage defect with a radius of 2 mm and a depth of 3 mm was established using a surgical drill. In the sham surgery group, the femoral trochlear joint surface was only exposed without inducing injury. Isotonic water was used to clean the wounds in all groups before suturing each layer. After the operation, each rabbit was kept in a separate cage and was free to drink and eat *ad libitum*. After modelling, continuous intramuscular injections of 4×10^6 U penicillin was used for 1 week.

A eukaryotic overexpression vector GV268-miR-330-3p was developed and injected 1 week after the operation in the intervention group. The modelling method was used as previously described.[22] The joint cavity was injected with GV268-independent sequence (control GV268-N-ODN; 15 μg of plasmid DNA dissolved in 0.5 ml of isotonic saline) in the model group and 0.5 ml of isotonic saline in the control group. Infusions were performed twice a week for 7 weeks and the synovial fluid was collected at the end of the 8th week. The rabbits were then anaesthetized with urethane (200 g/l, 5 ml/kg) and sacrificed by air embolization. The cartilage samples around the injured area were collected and divided into two parts: one part was used for polymerase chain reaction (PCR) analysis and the other was used for Western blot analyses.

ELISA detection

The collected synovial fluid was centrifuged at $2200 \times g$ for 10 min at 30°C using an Heraeus Megafuge™ 16 centrifuge (Thermo Fisher Scientific, Rockford, IL, USA) and the supernatant was collected. The supernatant was used for interleukin (IL)-1β (ab255730; Abcam®, Cambridge, MA, USA) and tumour necrosis factor (TNF)-α (ab31908; Abcam®) enzyme-linked immunosorbent assay (ELISA) detection. 100 μl of kit standard or synovial fluid sample was added to each well of a primary antibody-coated microplate from the kit. The samples were incubated for 2.5 h at room temperature. Then 100 μl of prepared biotinylated secondary antibody was added to each well and incubated for 1 h at room temperature. Then 100 μl of streptavidin solution was added to each well and incubated for 45 min at room temperature, followed by 100 μl of TMB One-Step Substrate Reagent to each well. The samples were incubated for 30 min at room temperature. Then 50 μl of Stop Solution was added to each well. A multifunctional microplate reader (Tecan M1000; Tecan, Männedorf, Switzerland) was used to measure the absorbance at a wavelength of 450nm. Three sets of wells were used for each condition and the entire experiment was performed in triplicate. The minimum detectable concentrations were 4.2 pg/ml for IL-1β and 4.8 pg/ml for TNF-α. Intra- and interassay

coefficients of variation for all ELISAs were <8% and <12%, respectively.

Western blot analyses

Total protein was extracted from 10 g of rabbit cartilage tissue using the RIPA lysis method (Shanghai Murphy, Shanghai, China). The protein concentration was determined using a BCA method kit (Shanghai Murphy). The proteins (0.5–17.5 μg per lane) were separated using 12% sodium dodecyl sulphate–polyacrylamide gel electrophoresis at 75 V for 30 min and then transferred to polyvinylidene fluoride membranes using electroblot apparatus at 80 V for 1 h (iBind™ Western Device; Thermo Fisher Scientific). The membranes were blocked using 2% bovine serum albumin (Thermo Fisher Scientific) at 30°C for 2 h, followed by incubation with the primary antibody (1:1000 dilution in Tris-buffered saline-Tween 20 [TBST; Thermo Fisher Scientific] pH 7.6; mouse/rat CD31/PECAM-1 antibody AF3628; R&D Systems, Minneapolis, MN, USA) for 2 h at 37°C. The membranes were washed three times with TBST (pH 7.6) at 22°C. Horseradish peroxidase-labelled goat anti-mouse secondary antibody (1:5000 dilution) was then added and the membranes were incubated at 37°C for 1 h and subsequently washed three times with TBST (pH 7.6) for 5 min each time. Enhanced chemiluminescence reagent (ab65623; Abcam®) was then added and it was allowed to develop in a dark room. The protein bands were scanned using a GS-900 Calibrated densitometer (Bio-Rad, Hercules, CA, USA) and the grey values were analysed using the Quantity One® software (version 4.6; Bio-Rad).

PCR analysis

Total RNA was extracted from 5 ml rabbit serum and 1 g cartilage tissue using TRIzol® reagent (Thermo Fisher Scientific). The purity, concentration and integrity of the total RNA were measured using UV spectrophotometry and agarose gel electrophoresis. cDNA was synthesized using the miScript II RT kit (Qiagen, Toronto, Canada) as per the manufacturer's instructions. The mature miR-330-3p expression level was quantified through quantitative real-time PCR using the mi-Script SYBR Green PCR kit (Qiagen) and miScript Primer Assay for SNORD61 and miR-330-3p (Qiagen) on the StepOnePlus Real-time PCR system (Life Technologies, Burlington, Canada). For gene expression, RNA was extracted using the RNeasy Mini kit (Qiagen) and cDNA synthesized using Omniscript RT kit (Qiagen) as per the manufacturer's instructions. The expression levels were quantified through quantitative real-time PCR using the QuantiTect SYBR Green PCR kit (Qiagen) on the StepOnePlus Real-time PCR system. The amplification conditions were as follows: 35 cycles of denaturation at 94°C for 1 min, annealing at 60°C for 1 min, chain extension at 72°C for 1 min, and a final extension step at 72°C for 10 min. MicroRNA expression levels were calculated using the comparative Ct method via StepOne Software (Life Technologies). The procedure was strictly conducted in accordance with the manufacturer's instructions. Three replicate wells were used for each sample and the entire experiment was performed in triplicate. U6 was used as an internal reference control. Data were analysed using the $2^{-\Delta ct}$ method. miR-330-3p primers and lentiviral vector were synthesized by Shanghai Shenggong Biotechnology (Shanghai, China) (Table 1).

Target gene prediction and dual luciferase assay

The online target gene prediction software Targetscan was used to identify a miRNA

Table 1. Primer sequences used for the polymerase chain reaction analysis.

Gene	Upstream primer	Downstream primer
miR-330-3p	5′-GCCAACAATATCCTGGTGCTG-3′	5′-CAGTGCAGGGTCCGAGGTAT-3′
U6	5′-CTCGCTTCGGCAGCACATA-3′	5′-CGAATTTGCGTGTCATCCT-3′

that can bind S100B as a target gene.[23] The 3′ UTRs of the wild type (S100B-WT) and mutant (S100B-MUT) forms of S100B were cloned and inserted downstream of the luc2 firefly luciferase gene of the pmiRGLO vector. Then these were co-transfected with the miR-330-3p-agomiR into 293T cells (American Type Culture Collection, Manassas, VA, USA). The 293T cells were maintained in Dulbecco's modified Eagle's medium (DMEM) supplemented with 10% fetal bovine serum and 1% penicillin/streptomycin at 37°C in 5% CO_2. The 293T cells were seeded a day prior to transfection at a density of 1×10^5 cells/ml in 1 ml of complete growth medium in each well of a 12-well tissue culture plate. DNA plasmids were incubated in serum-free DMEM complexed with Lipo2000 reagent at a ratio of 1:3 for 15 min and then added to cells. Equal total amounts of DNA were used in each transfected well by increasing total DNA with the appropriate empty vector plasmids. At 48 h after transfection, the 293T cells were lysed and the luciferase activity was measured using a dual luciferase assay kit (Promega, Madison, WI, USA). The luciferase activity of firefly and Renilla was measured by a microplate reader and standardized with Renilla luciferase.

Statistical analyses

All statistical analyses were performed using IBM SPSS Statistics for Windows, Version 20.0 (IBM Corp., Armonk, NY, USA) and GraphPad Prism 7 (Graphpad Software Inc., San Diego, CA, USA) was used to visualize the data. The categorical data are presented as frequencies (%) and compared using χ^2-test. The continuous data are presented as mean ± SD and compared using an independent sample *t*-test. Comparisons among the groups were analysed using analysis of variance and the Bonferroni test. The least significant difference *t*-test was used to test pairwise comparisons after the event. The Pearson correlation coefficient was used to test the relationship between miR-330-3p and S100B. A *P*-value of <0.05 was considered statistically significant.

Table 2. Comparison of the levels of interleukin (IL)-1β and tumour necrosis factor (TNF)-α in the synovial fluid from each group of rabbits.

Group	IL-1β, pg/ml	TNF-α, pg/ml
Control group	19.84 ± 3.05	117.29 ± 20.88
Model group	59.72 ± 7.69[a]	372.93 ± 42.34[a]
Intervention group	28.25 ± 4.88[a,b]	159.54 ± 25.74[a,b]
F-value	143.708	194.845
Statistical significance[c]	$P < 0.001$	$P < 0.001$

Data presented as mean ± SD.
[a]Compared with the control group, $P < 0.05$; [b]compared with the model group, $P < 0.05$.
[c]Compared using an independent sample *t*-test.

Results

The levels of IL-1β and TNF-α in the synovial fluid from the three groups of rabbits as measured by ELISA were significantly higher in the model group than in the intervention and control groups ($P < 0.05$ for all comparisons) (Table 2).

The levels of miR-330-3p in the cartilage tissue from the three groups of rabbits as measured by PCR analysis were significantly higher in the control group compared with the model group, but this level was significantly lower compared with the intervention group ($P < 0.001$ for both comparisons) (Figure 1). The level of miR-330-3p in the cartilage tissue was significantly higher in the intervention group compared with the model group ($P < 0.001$).

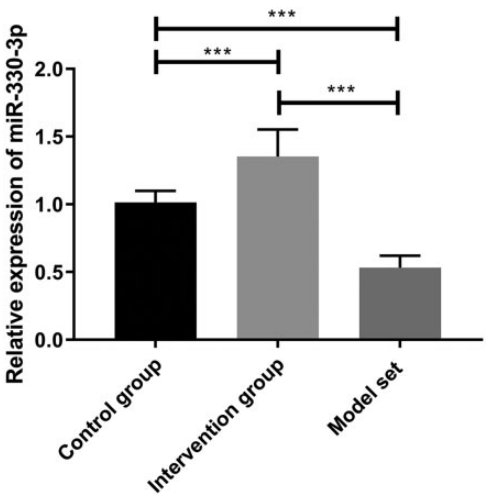

Figure 1. The levels of microRNA (miR)-330-3p in the cartilage tissue from each group of rabbits as measured by polymerase chain reaction analysis. Data presented as mean ± SD. ***$P < 0.001$; independent sample *t*-test.

The levels of S100B, FGFR1 and FGF-2 in the cartilage tissue from the three groups of rabbits as measured by Western blot analysis were significantly higher in the model group compared with the control and intervention groups ($P < 0.05$ for all comparisons) (Table 3). There were no significant differences in the levels of S100B, FGFR1 and FGF-2 between the intervention and control groups.

An analysis of the correlation between the levels of miR-330-3p and S100B in the intervention and model groups demonstrated an inverse correlation between miR-330-3p and S100B in both groups (model group: $r = -0.713$, $P = 0.016$; intervention group: $r = -0.735$, $P = 0.016$) (Table 4). A dual luciferase assay was used to determine the targeting relationship between miR-330-3p and S100B. The results demonstrated that miR-330-3p-agomiR significantly inhibited the fluorescence activity of S100B-WT (Figure 2), indicating that miR-330-3p targets and regulates S100B.

Table 4. Correlation analysis between the levels of microRNA (miR)-330-3p and S100 calcium-binding protein B (S100B).

Group	*r*-value	*P*-value
Intervention group	−0.735	$P = 0.016$
Model group	−0.731	$P = 0.016$

Table 3. The levels of S100 calcium-binding protein B (S100B), fibroblast growth factor receptor 1 (FGFR1) and fibroblast growth factor 2 (FGF-2) in the cartilage tissue from each group of rabbits as measured by Western blot analysis.

Group	S100B	FGFR1	FGF-2
Control group	0.537 ± 0.104	0.842 ± 0.142	0.725 ± 0.102
Model group	0.834 ± 0.184[a]	1.342 ± 0.284[a]	1.251 ± 0.173[a]
Intervention group	0.584 ± 0.112[b]	1.026 ± 0.181[b]	0.805 ± 0.125[b]
F-value	13.363	14.363	43.067
Statistical significance[c]	$P < 0.001$	$P < 0.001$	$P < 0.001$

Data presented as mean ± SD.
[a]Compared with the control group, $P < 0.05$; [b]compared with the model group, $P < 0.05$.
[c]Compared using an independent sample *t*-test.

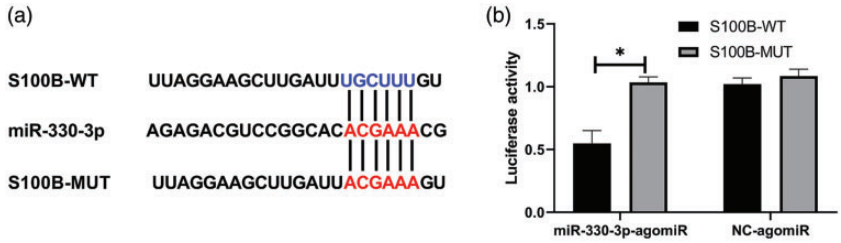

Figure 2. The target binding sites and mutation sites of microRNA (miR)-330-3p and S100 calcium-binding protein B (S100B) (a). Dual luciferase assay analysis of miR-330-3p and S100B targeted binding in 293T cells co-transfected with miR-330-3p-agomiR or NC-agomiR with S100B-wild type (S100B-WT) or S100B-mutant (S100B-MUT) (b). Data presented as mean ± SD. $^*P < 0.05$; independent sample *t*-test.

Discussion

Cartilage injury is normally caused by trauma.[24] The prevalence of cartilage injury is approximately 5% in the general population.[25]As cartilage tissue is integrated with vascular structures, its ability for self-repair is limited.[26] If the cartilage injury occurs without prompt treatment, the patient may develop OA, or traumatic arthritis, the most common of which is OA.[27,28]In the early stages of OA, clinicians mainly prescribe analgesics and anti-inflammatory drugs.[29] However, this only relieves the pain and does not prevent disease progression.[30] Joint replacement surgery is therefore a means to treat patients with the advanced OA.[31] If treatment intervention can be performed immediately after cartilage injury, the mental and economic burdens on patients can be reduced and their quality of life can be improved.[32]

This study measured the levels of miR-330-3p, S100B, FGFR1, FGF-2, TNF-α and IL-1β in cartilage tissue and synovial fluid of a rabbit model with cartilage injury. The levels of TNF-α and IL-1β in the synovial fluid of each group were measured using ELISA. As a mononuclear factor, TNF-α is produced by monocytes and macrophages.[33] TNF-α is found in infections, burns and malignant tumours.[34] Research has shown that TNF-α plays an important role in bone destruction.[35] It is also involved in the pathological processes of various forms of arthritis and intervention at the level of TNF-α can inhibit the progression of arthritis.[36] IL-1β and IL-17 are members of the interleukin family.[37] IL-1β acts as a pro-inflammatory cytokine.[38] When tissue is damaged or local oedema occurs, the level of IL-1β in the body increases rapidly.[39] Research has shown that IL-1β levels increase rapidly after bone injury.[40] The present study demonstrated that the levels of TNF-α and IL-1β in synovial fluid increased significantly following cartilage injury. This was likely because periosteal cells continue to engulf the cartilage destruction products in the synovial fluid after cartilage injury.[41] This causes a large amount of various inflammatory mediators to be secreted, leading to chronic inflammation.[41] At the same time, periosteal cells themselves can also secrete inflammatory mediators, further aggravating the inflammation.[41]

This current study also measured the levels of FGFR1, FGF-2 and S100B. As a transmembrane protein that regulates development, FGFR1 has an effect on the development of osteoblasts at different stages by binding to ligands.[42] Pericellular FGF-2 binds to perlecan, which is the heparan sulphate proteoglycan that sequesters FGF-2 in articular cartilage, where it

appears to play a functional role in chondrocyte mechanotransduction.[43] The role of FGF-2 is controversial in both articular and intervertebral disc (IVD) cartilage as it has been associated with species- and age-dependent anabolic or catabolic events.[44] FGF-2 selectively activates FGFR1 to exert catabolic effects in human articular chondrocytes and IVD tissue via upregulation of matrix degrading enzyme production, inhibition of extracellular matrix accumulation and proteoglycan synthesis.[44] In contrast, the administration of basic FGF into cartilaginous defects promotes the differentiation of chondrocytes and their matrix synthesis.[45] Research has shown that FGF-2 activation can promote the proliferation of bone marrow mesenchymal stem cells through the PI3K/Akt pathway, which can accelerate cartilage differentiation.[46] S100B belongs to the S100 calcium-binding protein family and plays an important role in cell differentiation, proliferation and apoptosis.[47] Research has shown that other S100 calcium-binding protein family members, S100A4, S100A8 and S100A11, are all involved in the process of articular cartilage repair.[48] This current study demonstrated that the levels of the FGFR1, FGF-2 and S100B proteins were significantly higher in the model group than in the control group, suggesting that the expression level of the S100B upstream target gene might be regulated to promote repair.

MicroRNAs are small non-coding RNAs of 21–25 nts in length.[49] The mRNAs of their targets can be degraded or translation of the protein can be inhibited when the miRNA is bound to the 3′-UTR of the target gene.[50] miR-330-3p is located on human chromosome 19.[51] Studies have shown that it has differential expression in a variety of digestive tract tumuors.[52,53] In this current study, Targetscan target gene prediction software was used to identify S100B as having a target site that could bind to miR-330-3p. Subsequently, a eukaryotic overexpression vector GV268-miR-330-3p was developed and injected into the animal models over 7 weeks. The level of miR-330-3p was significantly higher in the intervention group versus the control and model groups. The level of miR-330-3p was significantly lower in the model group compared with the control group. This indicated that miR-330-3p was expressed at low levels in injured cartilage tissues. The levels of FGFR1, FGF-2 and S100B protein were significantly lower in the intervention group compared with the model group, but there were no significant differences compared with the control group. The levels of TNF-α and IL-1β in the synovial fluid were significantly higher in the intervention group compared with the control group and significantly lower compared with the model group. There was an inverse correlation between miR-330-3p and S100B levels. The dual luciferase assay confirmed that S100B and miR-330-3p have a targeted regulatory relationship.

This current study had several limitations. First, the study did not specifically determine whether miR-330-3p binds directly to S100B in order to affect FGF-2/FGFR1 signalling. Secondly, the levels of miR-330-3p were determined by PCR, but the levels of FGFR1, FGF-2 and S100B mRNA were not assessed. It remains unclear whether these observations resulted from transcriptional or protein regulation. Therefore, studies are underway to better understand the relationship between miR-330-3p and S100B. Clinical trials should be conducted to verify the clinical significance of these results.

In conclusion, there may be a regulatory relationship between miR-330-3p and S100B. In this study, upregulation of miR-330-3p levels was found to reduce the levels of S100B and FGF-2/FGFR1 signalling appeared to be blocked.

Declaration of conflicting interest

The authors declare that there are no conflicts of interest.

Funding

This research received no specific grant from any funding agency in the public, commercial, or not-for-profit sectors.

ORCID iD

Dongming Liang https://orcid.org/0000-0001-6452-6544

References

1. Makris EA, Gomoll AH, Malizos KN, et al. Repair and tissue engineering techniques for articular cartilage. *Nat Rev Rheumatol* 2015; 11: 21–34.
2. van Dijk CN, Reilingh ML, Zengerink M, et al. Osteochondral defects in the ankle: why painful? *Knee Surg Sports Traumatol Arthrosc* 2010; 18: 570–580.
3. Song BW, Park JH, Kim B, et al. A Combinational Therapy of Articular Cartilage Defects: Rapid and Effective Regeneration by Using Low-Intensity Focused Ultrasound After Adipose Tissue-Derived Stem Cell Transplantation. *Tissue Eng Regen Med* 2020; 17: 313–322.
4. Jackson DW, Lalor PA, Aberman HM, et al. Spontaneous repair of full-thickness defects of articular cartilage in a goat model. A preliminary study. *J Bone Joint Surg Am* 2001; 83: 53–64.
5. Pap T and Korb-Pap A. Cartilage damage in osteoarthritis and rheumatoid arthritis–two unequal siblings. *Nat Rev Rheumatol* 2015; 11: 606–615.
6. Heijink A, Gomoll AH, Madry H, et al. Biomechanical considerations in the pathogenesis of osteoarthritis of the knee. *Knee Surg Sports Traumatol Arthrosc* 2012; 20: 423–435.
7. Tang X, Wang S, Zhan S, et al. The Prevalence of Symptomatic Knee Osteoarthritis in China: Results From the China Health and Retirement Longitudinal Study. *Arthritis Rheumatol* 2016; 68: 648–653.
8. Thomas GE, Palmer AJ, Batra RN, et al. Subclinical deformities of the hip are significant predictors of radiographic osteoarthritis and joint replacement in women. A 20 year longitudinal cohort study. *Osteoarthritis Cartilage* 2014; 22: 1504–1510.
9. Ouellet DL, Perron MP, Gobeil LA, et al. MicroRNAs in gene regulation: when the smallest governs it all. *J Biomed Biotechnol* 2006; 2006(4): 69616.
10. Zhang J, Li S, Li L, et al. Exosome and exosomal microRNA: trafficking, sorting, and function. *Genomics Proteomics Bioinformatics* 2015; 13: 17–24.
11. Rupaimoole R and Slack FJ. MicroRNA therapeutics: towards a new era for the management of cancer and other diseases. *Nat Rev Drug Discov* 2017; 16: 203–222.
12. Diaz-Romero J and Nesic D. S100A1 and S100B: Calcium Sensors at the Cross-Roads of Multiple Chondrogenic Pathways. *J Cell Physiol* 2017; 232: 1979–1987.
13. Choe N, Kwon DH, Shin S, et al. The microRNA miR-124 inhibits vascular smooth muscle cell proliferation by targeting S100 calcium-binding protein A4 (S100A4). *FEBS Lett* 2017; 591: 1041–1052.
14. Zhu L, Weng Z, Shen P, et al. S100B regulates inflammatory response during osteoarthritis via fibroblast growth factor receptor 1 signaling. *Mol Med Rep* 2018; 18: 4855–4864.
15. Roman-Blas JA and Jimenez SA. NF-kappaB as a potential therapeutic target in osteoarthritis and rheumatoid arthritis. *Osteoarthritis Cartilage* 2006; 14: 839–848.
16. Choi MC, Jo J, Park J, et al. NF-κB Signaling Pathways in Osteoarthritic Cartilage Destruction. *Cells* 2019; 8: 734.
17. Ye C, Ye J, Wu H, et al. Evidence of TWIST1 and transforming growth factor-β1 aberrant expressions as novel therapeutic targets in modulating the severity of osteoarthritis with focus on biologic agents. *J Physiol Pharmacol* 2020; 71: 825–832.
18. Korotkyi O, Huet A, Dvorshchenko K, et al. Probiotic Composition and Chondroitin Sulfate Regulate TLR-2/4-Mediated NF-κB Inflammatory Pathway and Cartilage Metabolism in Experimental Osteoarthritis. *Probiotics Antimicrob Proteins* 2021; 13: 1018–1032.

19. Korotkyi OH, Vovk A, Halenova TI, et al. Cytokines profile in knee cartilage of rats during monoiodoacetate-induced osteoarthritis and administration of probiotic. *Biopolymers and Cell* 2020; 36: 22–34.
20. American Psychological Association. Guidelines for ethical conduct in the care and use of animals. *J Exp Anal Behav* 1986; 45: 127–132.
21. Ren G, Whittaker JL, Leonard C, et al. CCL22 is a biomarker of cartilage injury and plays a functional role in chondrocyte apoptosis. *Cytokine* 2019; 115: 32–44.
22. Si HB, Zeng Y, Liu SY, et al. Intra-articular injection of microRNA-140 (miRNA-140) alleviates osteoarthritis (OA) progression by modulating extracellular matrix (ECM) homeostasis in rats. *Osteoarthritis Cartilage* 2017; 25: 1698–1707.
23. TargetScanHuman. Search for predicted microRNA targets in mammals, http://www.targetscan.org/vert_72/ (2018, assessed 22 June 2020).
24. Guilak F, Fermor B, Keefe FJ, et al. The role of biomechanics and inflammation in cartilage injury and repair. *Clin Orthop Relat Res* 2004; 423: 17–26.
25. Márquez WH, Gómez-Hoyos J, Gallo JA, et al. Prevalence of labrum and articular cartilage injuries of the hip on 3T magnetic resonance imaging of asymptomatic elite soccer players. *Rev Esp Cir Ortop Traumatol (Engl Ed)* 2019; 63: 77–85.
26. Ansari M and Eshghanmalek M. Biomaterials for repair and regeneration of the cartilage tissue. *Bio-Design and Manufacturing* 2018; 2: 41–49.
27. Jackson KA, Glyn-Jones S, Batt ME, et al. Assessing risk factors for early hip osteoarthritis in activity-related hip pain: a Delphi study. *BMJ Open* 2015; 5: e007609.
28. Jiménez G, Cobo-Molinos J, Antich C, et al. Osteoarthritis: Trauma vs Disease. *Adv Exp Med Biol* 2018; 1059: 63–83.
29. Yu RG, Zhang JY, Liu ZT, et al. Text Mining-Based Drug Discovery in Osteoarthritis. *J Healthc Eng* 2021; 2021: 6674744.
30. Messina OD, Vidal Wilman M and Vidal Neira LF. Nutrition, osteoarthritis and cartilage metabolism. *Aging Clin Exp Res* 2019; 31: 807–813.
31. Losina E, Paltiel AD, Weinstein AM, et al. Lifetime medical costs of knee osteoarthritis management in the United States: impact of extending indications for total knee arthroplasty. *Arthritis Care Res (Hoboken)* 2015; 67: 203–215.
32. Øiestad BE, Østerås N, Frobell R, et al. Efficacy of strength and aerobic exercise on patient-reported outcomes and structural changes in patients with knee osteoarthritis: study protocol for a randomized controlled trial. *BMC Musculoskelet Disord* 2013; 14: 266.
33. Awad AS, You H, Gao T, et al. Macrophage-derived tumor necrosis factor-α mediates diabetic renal injury. *Kidney Int* 2015; 88: 722–733.
34. Zhang N, Wang Q, Tian Y, et al. Expressions of IL-17 and TNF-α in patients with Hashimoto's disease combined with thyroid cancer before and after surgery and their relationship with prognosis. *Clin Transl Oncol* 2020; 22: 1280–1287.
35. Furman BD, Kimmerling KA, Zura RD, et al. Articular ankle fracture results in increased synovitis, synovial macrophage infiltration, and synovial fluid concentrations of inflammatory cytokines and chemokines. *Arthritis Rheumatol* 2015; 67: 1234–1239.
36. Kim HW, Lee CK, Cha HS, et al. Effect of anti-tumor necrosis factor alpha treatment of rheumatoid arthritis and chronic kidney disease. *Rheumatol Int* 2015; 35: 727–734.
37. Yazdi AS and Ghoreschi K. The Interleukin-1 Family. *Adv Exp Med Biol* 2016; 941: 21–29.
38. Patil T, More V, Rane D, et al. Pro-inflammatory cytokine Interleukin-1β (IL-1β) controls Leishmania infection. *Cytokine* 2018; 112: 27–31.
39. Zhang M, Zhou J, Wang L, et al. Caffeic acid reduces cutaneous tumor necrosis factor alpha (TNF-alpha), IL-6 and IL-1beta levels and ameliorates skin edema in acute and chronic model of cutaneous inflammation in mice. *Biol Pharm Bull* 2014; 37: 347–354.
40. Ruscitti P, Cipriani P, Carubbi F, et al. The role of IL-1beta in the bone loss during rheumatic diseases. *Mediators Inflamm* 2015; 2015: 782382.

41. Furman BD, Mangiapani DS, Zeitler E, et al. Targeting pro-inflammatory cytokines following joint injury: acute intra-articular inhibition of interleukin-1 following knee injury prevents post-traumatic arthritis. *Arthritis Res Ther* 2014; 16: R134.
42. Jacob AL, Smith C, Partanen J, et al. Fibroblast growth factor receptor 1 signaling in the osteo-chondrogenic cell lineage regulates sequential steps of osteoblast maturation. *Dev Biol* 2006; 296: 315–328.
43. Vincent TL, McLean CJ, Full LE, et al. FGF-2 is bound to perlecan in the pericellular matrix of articular cartilage, where it acts as a chondrocyte mechanotransducer. *Osteoarthritis Cartilage* 2007; 15: 752–763.
44. Ellman MB, Yan D, Ahmadinia K, et al. Fibroblast growth factor control of cartilage homeostasis. *J Cell Biochem* 2013; 114: 735–742.
45. Fujimoto E, Ochi M, Kato Y, et al. Beneficial effect of basic fibroblast growth factor on the repair of full-thickness defects in rabbit articular cartilage. *Arch Orthop Trauma Surg* 1999; 119: 139–145.
46. Yun YR, Jang JH, Jeon E, et al. Administration of growth factors for bone regeneration. *Regen Med* 2012; 7: 369–385.
47. Tsoporis JN, Mohammadzadeh F, Parker TG. S100B: a multifunctional role in cardiovascular pathophysiology. *Amino Acids* 2011; 41: 843–847.
48. Yammani RR. S100 proteins in cartilage: role in arthritis. *Biochim Biophys Acta* 2012; 1822: 600–606.
49. Ullah Y, Li C, Li X, et al. Identification and Profiling of Pituitary microRNAs of Sheep during Anestrus and Estrus Stages. *Animals (Basel)* 2020; 10: 402.
50. Ha M and Kim VN. Regulation of microRNA biogenesis. *Nat Rev Mol Cell Biol* 2014; 15: 509–524.
51. Roy B, Wang Q, Palkovits M, et al. Altered miRNA expression network in locus coeruleus of depressed suicide subjects. *Sci Rep* 2017; 7: 4387.
52. Guan A, Wang H, Li X, et al. MiR-330-3p inhibits gastric cancer progression through targeting MSI1. *Am J Transl Res* 2016; 8: 4802–4811.
53. Meng H, Wang K, Chen X, et al. MicroRNA-330-3p functions as an oncogene in human esophageal cancer by targeting programmed cell death 4. *Am J Cancer Res* 2015; 5: 1062–1075.